Instability behaviour of Changi sand in plane-strain tests

Instabilité de comportement de sable Changi lors d'essais en déformation plane

D. Wanatowski
Nottingham Centre for Geomechanics, Faculty of Engineering, University of Nottingham, United Kingdom
J. Chu
School of Civil and Environmental Engineering, Nanyang Technological University, Singapore

ABSTRACT
Flowslide is a common type of failure of granular soil slopes. Although many flowslides can be explained using static liquefaction or instability behaviour of sand under undrained conditions, some of the failures might have occurred under essentially drained conditions, e.g. the Wachusett Dam case in 1907. Recent laboratory studies on Changi sand under axisymmetric conditions have shown that sand can become unstable under completely drained conditions. Based on these laboratory studies, new failure mechanisms for granular slopes were proposed. However, to date, most of the experiments on the instability behaviour of granular soils were carried out under axisymmetric conditions even though slope failures can only be simplified into plane-strain conditions. Although the behaviour of sand under plane-strain conditions has been studied by a number of researchers, the instability of sand under plane-strain conditions has seldom been investigated. In this paper, experimental data obtained from plane-strain tests are presented to illustrate the unstable behaviour of sand under both undrained and drained conditions. A comparison between the instability conditions observed under axisymmetric and plane-strain conditions is made. A unified instability condition which is applicable to both axisymmetric and plane-strain conditions is presented.

RÉSUMÉ
Le glissement par liquéfaction est un type commun de rupture des pentes des sols granulaires. Bien que de nombreux glissements par liquéfaction peuvent être expliqués en utilisant la liquéfaction statique ou le comportement d'instabilité du sable en conditions non-drainées, il se pourrait que certaines ruptures se soient produites en conditions essentiellement drainées, comme par exemple dans le cas du barrage de Wachusett en 1907. De récentes études de laboratoire sur du sable Changi sous conditions axisymétriques ont montré que le sable peut devenir instable en conditions de drainage complet. De nouveaux mécanismes de rupture de pentes granulaires ont été proposés en se basant sur ces études de laboratoire. Cependant, la plupart des expériences sur le comportement d'instabilité des sols granulaires ont jusqu'à présent été conduites en conditions axisymétriques alors que les ruptures de pente peuvent être simplifiées uniquement en conditions de déformations planes. Bien que le comportement du sable en conditions de déformations planes ait été étudié par nombre de chercheurs, l'instabilité du sable en conditions de déformations planes a rarement été examinée. Des données expérimentales obtenues à partir de tests en déformations planes sont présentées dans cet article pour illustrer le comportement instable du sable en conditions à la fois non-drainées et drainées. Les caractéristiques d'instabilité observées en conditions d'axisymétrie et de déformations planes sont comparées. Une condition d'instabilité unifiée applicable en conditions à la fois d'axisymétrie et de déformations planes est présentée.

Keywords : stress-strain behaviour, failure, laboratory tests, sands, slopes, plane-strain

1 INTRODUCTION

Flowslide is a common type of failure of granular soil slopes. Static liquefaction (or instability) is considered to be one of the main triggering factors causing flowslides. Although it is a common understanding that static liquefaction only occurs for loose granular material under undrained conditions, there are cases where failure of granular slopes occurred under other drainage conditions. For example, in the reanalysis of the Wachusett Dam case in 1907, Olson et al. (2000) concluded that the failure was caused by static liquefaction under completely drained conditions.

Several experimental studies on instability behaviour of sand under drained conditions have been reported in the past (e.g. Chu et al. 2003). However, most of the studies were carried out under axisymmetric conditions. As most of the failures are in plane-strain, instability behaviour should be studied under plane-strain conditions. Although the behaviour of sand under plane-strain conditions have been studied before (e.g., Han and Vardoulakis 1991; Alshibli et al. 2003), instability of sand under plane-strain conditions has not been investigated in detail.

The objectives of this paper are to study the instability behaviour of Changi sand under plane-strain conditions, and to verify whether the findings on instability established based on triaxial tests are applicable to plane-strain problems.

2 EXPERIMENTAL STUDY

2.1 *Material tested*

The soil tested in this study was a marine dredged silica sand, the so-called Changi sand, used for the Changi land reclamation project in Singapore. Changi sand contains approximately 12% of shells and has been used in a number of experimental studies. Its index properties are given in Wanatowski & Chu (2006).

2.2 *Testing arrangement*

All tests were performed in a plane-strain apparatus developed by Wanatowski & Chu (2006). The plane-strain condition was imposed by two metal vertical platens, fixed in position by two pairs of horizontal tie rods. The lateral stress in the ε_2=0 direction (i.e. intermediate principal stress, σ_2) was measured by four submersible pressure cells with two on each vertical platen.

The plane-strain testing system was fully automated. A digital hydraulic force actuator was mounted at the bottom of a

Proceedings of the 17th International Conference on Soil Mechanics and Geotechnical Engineering
M. Hamza et al. (Eds.)

doi:10.3233/978-1-60750-031-5-89

loading frame to apply axial load. The actuator was controlled by a computer via a digital load/displacement control box. The control box adjusted the movement of the base pedestal to achieve a desired rate of load or rate of displacement so that either deformation-controlled or load-controlled loading mode could be applied. The vertical load was measured by an internal load cell.

A pair of miniature submersible linear variable differential transformers (LVDT) was used to measure the vertical displacement. An external LVDT was also used to measure the axial strain when the internal LVDTs run out of travel. The cell pressure was applied through a digital pressure/volume controller (DPVC). Another DPVC was used to control the back pressure from the bottom of the specimen while measuring the volumetric change at the same time. For details of the testing arrangement, see Wanatowski & Chu (2006).

2.3 *Specimen preparation and testing procedures*

The water sedimentation (WS) and the moist tamping (MT) methods were adopted in the preparation of specimens. The WS method was used for medium loose and medium dense specimens, while the MT method was used for very loose and loose specimens. The dimensions of the prismatic specimen were 120 mm in height and 60 × 60 mm in cross-section. Free ends with enlarged platens were used to minimize end restraint; whereas bedding and membrane penetration errors were reduced to an insignificant value by using the liquid rubber technique developed by Lo et al. (1989).

For saturation, the specimen was flushed with de-aired water from the bottom to the top for around 60 minutes under a water head of about 0.5 m. After that, a back-pressure of 400 kPa was applied to ensure a B-value of at least 0.96 was achieved, thus indicating a high degree of saturation.

All the specimens were consolidated from an initial isotropic stress state of 20 kPa to the required stress state along the K_0 path. The K_0 condition was achieved by controlling $d\varepsilon_v/d\varepsilon_1 = 1$ using a strain path method described by Lo & Chu (1991).

Two types of instability test were conducted in this study. Undrained instability tests were carried out by maintaining a constant deviatoric stress with drainage valves closed. Drained instability tests were conducted under a fully drained condition along a stress path with constant deviatoric stress, but decreasing mean effective stress. This type of stress path is referred to as a constant shear-drained (CSD) test (Brand 1981, Chu et al. 2003). The mean effective stress was reduced by increasing the back pressure while maintaining the confining pressure constant. The back pressure was increased through a DPVC at a rate of 0.5 kPa/min while maintaining the axial load constant. This rate was selected to ensure pressure equilibrium within the specimen during the test.

3 RESULTS

Only representative test results are presented in this paper and the deviatoric stress q and the mean effective stress p' are defined by Eqs (1) and (2), respectively.

$$q = \frac{1}{\sqrt{2}}\left[\left(\sigma_1 - \sigma_2\right)^2 + \left(\sigma_2 - \sigma_3\right)^2 + \left(\sigma_3 - \sigma_1\right)^2\right]^{1/2} \quad (1)$$

$$p' = \frac{1}{3}\left(\sigma_1' + \sigma_2' + \sigma_3'\right) \quad (2)$$

where σ_1, σ_2, and σ_3 are major, intermediate, and minor principal stresses, respectively. The prime refers to the effective stress.

3.1 *Undrained behaviour*

The results of three instability tests INU01, INU02, and INU03, carried out under plane-strain conditions, are presented in Fig. 1. Test INU01 was performed by shearing the specimen from the K_0 condition (point A_1) to an effective stress ratio of q/p' = 1.04 (point B_1) along a drained path, as shown in Fig. 1(a). Upon reaching point B_1, an undrained condition was imposed while the deviatoric stress was kept constant. The void ratio at point B_1 was e = 0.889. The instability line (IL) corresponding to e = 0.888 as determined by the CK_0U plane-strain tests conducted on very loose sand (Wanatowski & Chu 2007) is also plotted in Fig. 1(a). The IL was determined by a line connecting the peaks of a series of effective stress paths obtained from CK_0U tests using Lade's method (Lade 1992).

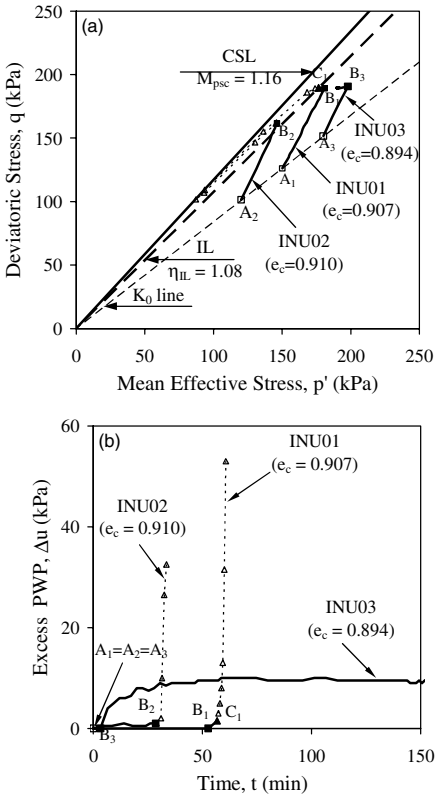

Figure 1. Instability of loose sand under undrained conditions: (a) effective stress paths; (b) excess pore water pressure against time curves.

The excess pore water pressure developed during the instability tests are shown in Fig. 1(b). It can be seen from Fig. 1(b) that in Test INU01, the pore water pressure started to increase immediately after drainage conditions were changed from drained to undrained at point B_1. Within next few minutes the pore water pressure shot up and instability occurred at point C_1. This was accompanied by a sudden increase in ε_1 rate (Wanatowski 2005). The effective stress at point C_1 is shown in Fig. 1(a). It can be seen that C_1 is close to the IL determined by CK_0U tests on loose Changi sand (Wanatowski & Chu 2007). When instability occurred at point C_1, the specimen physically collapsed.

Test INU02 was conducted in a way similar to Test INU01. After K_0 consolidation the stress state was brought to point B_2 (q/p' = 1.11). The void ratio at point B_2 was e = 0.888. It can be seen from Fig. 1(a) that point B_2 is slightly above the IL, corresponding to e = 0.888. Upon reaching point B_2, the deviatoric stress was maintained constant and an undrained condition was imposed. Under such conditions, the pore water pressure increased rapidly at point B_2, as shown in Fig. 1(b). This was again accompanied by a sudden increase in ε_1 rate

(Wanatowski 2005).The instability occurred and the specimen physically collapsed.

Test INU03 was carried out in a way similar to Test IND02, except that the consolidation stresses were higher. As shown in Fig. 1(a), the specimen was brought from point A_3 to point B_3 along a drained path. The deviatoric stress at point B_3 is the same as that in Test INU01 (q = 190 kPa). However, in terms of effective stress ratio, the q/p' at point B_3 is 0.96, which is lower than that at point B_1 (Test INU01). The void ratio at B_3 is 0.886. Upon reaching point B_3, the deviatoric stress was kept constant and an undrained condition was imposed. During a period of 150 min, the pore water pressure (Fig. 1(b)) and the axial strain (Wanatowski 2005) did not change much. The specimen was at a stable state.

The results of the above three tests indicate that the undrained instability can occur for very loose sand under plane-strain conditions. The occurrence of undrained instability appears to be controlled by the stress ratio $\eta = q/p'$. When η reaches the η of the instability line, that is η_{IL}, instability occurs, as in Tests INU01 and INU02. However, if η is much smaller than η_{IL}, instability will not occur. This observation is consistent with that made in triaxial tests by Leong & Chu (2002) and Chu et al. (2003).

3.2 *Drained behaviour*

The results of two typical drained instability tests, IND01 and IND03, conducted on very loose and very dense sand respectively are presented in Fig. 2. The specimens were anisotropically consolidated to the mean effective stresses of 200 kPa and 206 kPa (points A_1 and A_3). The void ratios of the specimens after consolidation were e_c = 0.902 and 0.679, respectively. After consolidation the specimens were sheared along constant shear drained (CSD) paths.

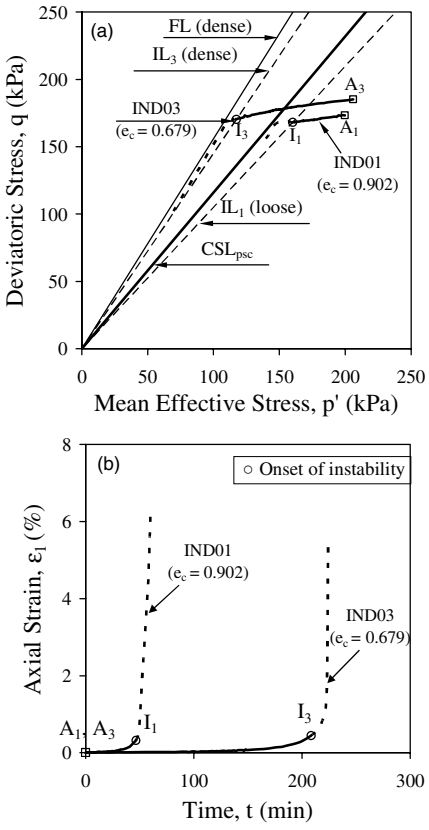

Figure 2. Instability of loose and dense sand under drained conditions: (a) effective stress paths; (b) axial strain against time curves.

The effective stress paths obtained from the two tests are plotted in Fig. 2(a). The critical state line (CSL) and the failure line (FL) as defined by drained plane-strain tests (Wanatowski & Chu 2006) are also plotted in Fig. 2(a). It can be seen that due to the reduction of the mean effective stress, the effective stress paths moved from points A_1 and A_3 to points I_1 and I_3, respectively. The change in axial strain with time for the two tests is presented in Fig. 2(b). It can be seen from Fig. 2(b) that between points A_1, A_3 and I_1, I_3 there was a little axial strain developed in both tests. When the stress states reached points I_1 and I_3, the axial strains in both tests started to develop at faster rates, as shown in Fig. 2(b). Therefore, according to the definition given by Chu et al. (2003), instability occurred at points I_1 and I_3. These points can be used to determine instability lines, IL_1 and IL_3 corresponding to e_c = 0.902 and 0.679, respectively, as shown in Fig. 2(a).

It can be seen from Fig 2(a) that instability occurred much earlier in the loose specimen than in the dense specimen. The loose specimen became unstable before reaching the CSL. On the other hand, the medium dense specimen became unstable after the CSL, but before reaching the FL. However, the CSL is also the FL for loose sand. Therefore, pre-failure instability occurred in both tests. Furthermore, the pore water pressures did not change during the two tests (Wanatowski 2005). Therefore, instability in a form of a rapid increase in plastic strains occurred in loose and dense sand under fully drained conditions.

4 DISCUSSION

The results of plane-strain tests reported in this paper indicate that the undrained instability occurs for very loose sand under plane-strain conditions in a way similar to that under axisymmetric conditions. Similar to triaxial tests, when undrained instability occurs in plane-strain tests, the specimen physically collapses. This suggests that the conditions for the occurrence of the instability are the same for both plane-strain and triaxial tests. i.e., the stress state needs to be above the IL.

As explained by Chu et al. (2003) the IL under axisymmetric conditions is defined based on yielding conditions. For contractive sand, the slope of instability line, η_{IL}, can be determined by connecting the peaks of the undrained stress paths (Lade 1992). For dilative sand, the effective stress path of an undrained test will increase monotonically and approach the constant stress ratio line (CSRL), which can be used to determine the η_{IL}. The IL defined in this way specifies a yielding where large plastic strains can develop (Chu et al. 2003).

Based on the results obtained from medium dense specimens (Wanatowski 2005) and the results obtained from very loose specimens (Wanatowski & Chu 2007), the slope of the IL, η_{IL}, is plotted against a modified state parameter, $\bar{\psi}$, in Fig. 3. The $\bar{\psi}$ is defined by Chu et al. (2003) as:

$$\bar{\psi} = e_{IL} - e_{cs} \tag{3}$$

where e_{IL} is the void ratio at the instability state and e_{cs} is the void ratio at the critical state under the same mean effective stress. The difference between the modified state parameter $\bar{\psi}$ and the state parameter ψ defined by Been & Jefferies (1985) is that the $\bar{\psi}$ defines the state at the instability line rather than the state after consolidation, as proposed by Been & Jefferies (1985). This means that the $\bar{\psi}$ can be used for both undrained and drained conditions, which facilitate the application of the state parameter concept to slope stability analysis.

Figure 3 shows that a unique relationship between the η_{IL} and $\bar{\psi}$ exists for both plane-strain and triaxial tests. However, in order to obtain a single curve in Fig. 3 for both triaxial and plane-strain tests, the η_{IL} must be normalised using the slope of the CSL, M, and the η_{IL}/M must be plotted against $\bar{\psi}$. This is because the CSL determined under plane-strain test conditions is different from that under axisymmetric conditions on both q–p' and e–p' planes (Wanatowski & Chu 2006). Therefore, the

$\overline{\psi}$ value under axisymmetric conditions is different from that under plane-strain conditions for a specimen with the same void ratio and mean effective stress. The difference in CSL is related to effect of the intermediate principal stress (σ_2), as discussed by Wanatowski & Chu (2007). As shown in Fig. 3, the η_{IL}/M–$\overline{\psi}$ relationship is not affected by the σ_2. This implies that the framework of instability line for sand established under axisymmetric conditions is applicable to plane-strain problems.

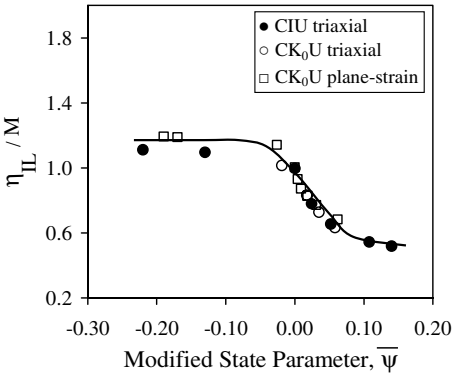

Figure 3. Relationship between the slope of instability line and the modified state parameter established for triaxial and plane-strain tests.

The plane-strain test results presented in the preceding section showed that instability can take place for both loose and dense sand under drained conditions. This is consistent with previous experimental studies conducted under axisymmetric conditions (Chu & Leong 2001; Chu et al. 2003).

As explained earlier, the IL under axisymmetric conditions is defined based on yielding conditions. This implies that the IL that controls the occurrence of instability is the same for both drained and undrained conditions. To verify this assumption, the η_{IL}/M versus $\overline{\psi}$ curve obtained in Fig. 3, is replotted in Fig. 4 together with the instability points obtained from plane-strain tests conducted under drained conditions. It can be seen from Fig. 4 that the η_{IL} obtained from drained instability tests agrees well with that determined from undrained tests. Therefore, the η_{IL} obtained from undrained tests can be used to predict the instability under drained conditions. As shown in Fig. 4 the η_{IL} on the contractive side ($\overline{\psi} > 0$) changes more drastically than η_{IL} on the dilative side ($\overline{\psi} < 0$). This is consistent with the observation made under axisymmetric conditions that the influence of void ratio on the unstable behaviour of loose sand is much greater than that on the behaviour of dense sand (Chu et al. 2003).

5 CONCLUSIONS

K_0 consolidated undrained and drained instability tests were conducted on Changi sand using a plane-strain apparatus. The following conclusions can be drawn from the study:

1. When loose sand is tested under an undrained condition using the plane-strain apparatus, the undrained instability can occur. This is consistent with the experimental results obtained under axisymmetric conditions.
2. Both contractive and dilative sand specimens can become unstable under a drained condition. This is consistent with the experimental results obtained under axisymmetric conditions.
3. The instability line defined based on yielding conditions is the same for both drained and undrained tests and defines the lower bound of all the possible unstable states regardless of the drainage conditions. Therefore, instability can occur under either undrained or drained conditions as long as the stress state falls above the instability line.
4. When the slope of instability line, η_{IL}, is normalized by the slope of the CSL, M, a unique relationship between η_{IL}/M and $\overline{\psi}$ can be obtained for both axisymmetric and plane-strain conditions. Using this relationship, the instability conditions established in triaxial tests can be used for plane-strain problems. As a result, a framework formulated by Chu et al. (2003) for axisymmetric conditions using the modified state parameter $\overline{\psi}$ and the CSL can be extended into plane-strain conditions.

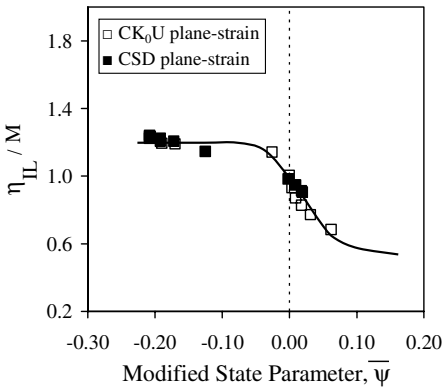

Figure 4. Comparison of slopes of the instability line obtained from undrained and drained plane-strain instability tests.

REFERENCES

Alshibli, A.K., Batiste, S.N. & Sture, S. 2003. Strain localization in sand: plane strain versus triaxial compression. *Journal of Geotechnical and Geoenvironmental Engineering* 129(6): 483-494.

Been, K. & Jefferies, M.G. 1985. A state parameter for sand. *Géotechnique* 35(2): 99-112.

Brand, E.W. 1981. Some thoughts on rain-induced slope failures. In *Proceedings of the 10th International Conference on Soil Mechanics and Foundation Engineering,* Stockholm, Vol. 3, pp. 373-376.

Chu, J. & Leong, W.K. 2001. Pre-failure strain softening and pre-failure instability of sand: a comparative study. *Géotechnique* 51(4): 311-321.

Chu, J., Leroueil, S. & Leong, W.K. 2003. Unstable behaviour of sand and its implication for slope stability. *Canadian Geotechnical Journal* 40: 873-885.

Han, C. & Vardoulakis, I.G. 1991. Plane-strain compression experiments on water-saturated fine-grained sand. *Géotechnique* 41(1): 49-78.

Lade, P.V. 1992. Static instability and liquefaction of loose fine sandy slopes. *Journal of Geotechnical Engineering* 118(1): 51-71.

Leong, W.K. & Chu, J. 2002. Effect of undrained creep on instability behaviour of loose sand. *Canadian Geotechnical Journal* 39: 1399-1405.

Lo, S.-C.R., Chu, J. & Lee, I.K. 1989. A technique for reducing membrane penetration and bedding errors. *Geotechnical Testing Journal* 12(4): 311-316.

Lo, S.-C.R. & Chu, J. 1991. The measurement of K_0 by triaxial strain path testing. *Soils and Foundations* 31(2): 181-187.

Olson, S. M., Stark, T.D., Walton, W.H. & Castro, G. (2000). 1907 Static Liquefaction Flow Failure of the North Dike of Wachusett Dam. *Journal of Geotechnical and Geoenvironmental Engineering* 126(12): 1184-1193.

Wanatowski, D. 2005. *Strain softening and instability of sand under plane-strain conditions.* Ph.D. thesis, Nanyang Technological University, Singapore.

Wanatowski, D. & Chu, J. 2006. Stress-strain behavior of a granular fill measured by a new plane-strain apparatus. *Geotechnical Testing Journal* 29(2): 149-157.

Wanatowski, D. & Chu, J. 2007. Static liquefaction of sand in plane-strain. *Canadian Geotechnical Journal* 44(3): 299-313.